Identifying sediment sources by applying a fingerprinting mixing model in a Pyrenean drainage catchment

Leticia Palazón • Leticia Gaspar • Borja Latorre • William H. Blake • Ana Navas

L. Palazón (✉) • B. Latorre • A. Navas
Department of Soil and Water. Estación Experimental de Aula Dei (EEAD-CSIC), Avda. Montañana 1005, Zaragoza, 50059, Spain

L. Gaspar • W. H. Blake
School of Geography, Earth and Environmental Sciences, Plymouth University, Plymouth, Devon, PL4 8AA, UK

(✉) **Corresponding author:**
Tel.: +34 976 71 61 43
Fax: +34 976 71 61 45
Leticia Palazón
e-mail: lpalazon@eead.csic.es

Abstract

Purpose: Spanish Pyrenean reservoirs are under pressure from high sediment yields in their contributing catchments. Sediment fingerprinting approaches offer the potential to quantify the contribution of different sediment sources, evaluate catchment erosion dynamics and develop management plans to tackle, among other problems, reservoir siltation. Within this context, the objective of this study was to assess catchment source contribution changes both over a longitudinal river reach and to a reservoir delta deposit to improve our understanding of sediment supply dynamics.

Materials and methods: The catchment of the Isábena River (445 km^2), located in the central Spanish Pyrenees, is an agroforest catchment supplying sediments, together with the Ésera River, to the Barasona reservoir at an annual rate of ~350 t km^2 with implications for reservoir longevity. The ability to discriminate between agricultural, forest, subsoil and scrubland sources of geochemical, radionuclide and magnetic susceptibility fingerprint properties analysed in the <63 μm sediment fraction was investigated by conducting statistical tests to select an optimum composite fingerprint. The contributions of sediment sources for channel bed and delta sediments were assessed by applying a new data processing methodology which was written in the C programming language and designed to test the entire parameter space, providing a detailed description of the optimal solution by a Monte Carlo method.

Results and discussion: The solution for each sample was characterised by the mean value of the user-defined solutions (n = 100) and the lower goodness of fit value applied. The solutions from the mixing model had goodness of fit values >82 %. The channel bed sediments in the upper reach were dominated by subsoil sources (>80 %), and the lower reaches had a higher proportion of sediment coming from agricultural source (>55 %). Contributions for delta sediments were dominated by agricultural, forest and subsoil sources but in varying proportions within the deposit. The switch in the sources of sediment between the headwaters and the catchment outlet was due to differences in the distribution of the land uses/land covers in the contributing areas. Differences between channel bed sediment and delta sediment source contributions were related to local sediment deposition conditions.

Conclusions: The new unmixing approach is able to provide the optimal solution by a robust and integral Monte Carlo method guaranteeing a broader interpretation of the optimal solution including its dispersion in all unmixing cases. The results support the use of sediment fingerprinting approaches in this Spanish Pyrenees mountain catchment, which will enable us to better understand catchment sediment delivery to an important water supply reservoir.

Keywords: Mixing model • Mountain catchment • Sediment fingerprinting • Spanish Pyrenees

1 Introduction

Concern for the impact of accelerated rates of soil erosion on agricultural land, resulting from land clearance and poor land management, has traditionally focused on their effects in terms of soil degradation, reduced crop productivity, problems of food security and destruction of an essentially non-renewable resource (e.g. Wischmeier and Smith 1978; Evans and Boardman 1994; Lal 1998; Minella et al. 2008). These effects are often termed on-site impacts. Increasingly, attention has also been directed to the equally important, and perhaps even more significant, off-site impacts. These include a wide spectrum of potential impacts, which range from reservoir siltation to the role of sediment as a diffuse source pollutant (e.g. Waters 1995; Wood and Armitage 1997, 1999; Acornley and Sear 1999; Walling et al. 2003; Minella et al. 2008). Sediment has a variety of roles and impacts and its regulation and management are complex. In this context, reservoir siltation presents a critical off-site problem derived from soil erosion and sediment delivery within the Mediterranean environment (Navas et al. 2004), and its effects can be economically and societally serious both in terms of both water and energy security. Reservoir siltation is a concern for most reservoirs in the Mediterranean region but particularly for those in mountainous areas, where high erosion rates rapidly reduce the storage capacity of reservoirs (Navas et al. 2011).

In mountainous environments, the problems associated with sedimentation are exacerbated by the fact that the bulk of the sediment is exported within very short periods, after violent storms or during the annual snowmelt (Meybeck et al. 2003). Mano et al. (2009) showed that 40–80% of the annual flux of suspended sediment occurred within 2 % of the time in four Alpine catchments. Major erosion events need to be anticipated – e.g. by improving reservoir management – or even controlled in upstream reaches and hillslopes to prevent downstream problems (Evrard et al. 2011). Hence, information on water-induced soil erosion and sediment export in mountain areas is essential in order to implement management practices designed to prevent reservoir siltation (Molino et al. 2007).

Traditional methods of sediment provenance assessment (e.g. erosion mapping, surveying using profilometers or erosion pins, erosion vulnerability indices or erosion plots) are commonly constrained by problems of representativeness and high costs, limiting the spatial coverage and monitoring duration of many methods (Peart and Walling 1986; Collins and Walling 2004). An efficient and direct way to determine the

sediment sources within a catchment is by adopting sediment fingerprinting techniques. Thus, sediment fingerprinting investigations have expanded and developed greatly over the past three decades (e.g. Davis and Fox 2009; Collins et al. 2010b; Mukundan et al. 2012; Koiter et al. 2013; Smith and Blake 2014) in response to a growing need for information on sediment sources and to technological advances which facilitate such work (Walling 2013). However, source fingerprinting techniques continue to be most widely applied in agricultural and forest catchments (e.g. Owens et al. 2000; Collins et al. 2010b; Martínez-Carreras et al. 2010a, b, c; Blake et al. 2012; Schuller et al. 2013) and application in mountainous catchments is limited (Evrard et al. 2011). Sediment fingerprinting usually employs a combination of natural sediment properties as tracers ('fingerprints') collected from both potential source areas and sediment samples that commonly represent mixtures of sources (Walling 2005). It is founded upon two principal assumptions: (1) that the selected fingerprints maintain their properties during sediment mobilisation and transportation processes allowing discrimination of potential sources and (2) that comparison of source and sediment material using these fingerprints permits determination of relative source contribution (Collins and Walling 2004). Thereby, sources are commonly defined either spatially (e.g. tributary sub-catchments, geological sub-areas) or typologically (e.g. land use types, surface vs. sub-surface sources) (Collins and Walling 2002). Investigations have shown that a range of characteristic soil properties can be used as fingerprints to trace back the sources of river sediments, including mineral magnetism (e.g. Yu and Oldfield 1989; Walden et al. 1997), colour (e.g. Grimshaw and Lewin 1980; Krein et al. 2003; Martínez-Carreras et al. 2010a, b, c), geochemical composition (Olley and Caitcheon 2000; Haddadchi et al. 2014), environmental radionuclides (e.g. Motha et al. 2003; Minella et al. 2008; Navratil et al. 2012; Owens et al. 2012) and, more recently, Compound Specific Stable Isotopes (CSSIs) (Gibbs 2008; Blake et al. 2012; Hancock and Revill 2013). The use of composite fingerprints, employing several diagnostic properties, has proven to be reliable (e.g. Collins et al. 1997). However, due to the wide range of potential controls on sediment properties, there is no universal recommendation on which properties to include, making parameter retrieval and data exploration often time-consuming and costly (e.g. Collins and Walling 2002).

Sediment fingerprinting studies often rely on the collection of suspended sediment from different flood events or varying times within a flood (Mizugaki et al. 2008; Devereux

et al. 2010; Mukundan et al. 2010; Navratil et al. 2012; Smith and Blake 2014) However, a spatially distributed monitoring network for suspended sediments is difficult to set up and very expensive to have in each river catchment. Fingerprinting studies have also been successfully applied to river bed sediments (Olley and Caitcheon 2000; Dirszowsky 2004; Hughes et al. 2009; Evrard et al. 2011; Schuller et al. 2013), wherein it should be noted that sediment storage dynamics are an important consideration.

In this study, we aim to apply a fine sediment source fingerprinting procedure to discriminate land use/land cover sources in the Isábena River catchment (Spanish Pyrenees) that are hypothesised to contribute to the infilling of the Barasona reservoir by fine sediment. In this context, we analysed grain size fractions, organic carbon content, mass activities of environmental radionuclides, magnetic susceptibility and geochemistry to investigate the ability of the obtained fingerprints for discriminating between cultivated, forest, scrubland and subsoil sources. The obtained optimum composite fingerprint was used to apply a mixing model to evaluate source contributions for sediment deposited in channel beds and in a terminal delta at the outflow of the Isábena River into the reservoir. As the optimization process used to solve the mixing model is considered a stage of critical importance, this was implemented by a new Monte Carlo method designed to test the entire parameter space providing a detailed description of the optimal solution. The specific objectives were (i) to identify the physical and chemical basis for source discrimination by tracer properties selected using the fingerprinting procedure and (ii) to assess source contributions for sediment samples collected from the channel beds and a reservoir delta deposit.

2 Material and methods

2.1 Study area

The Isábena River, located in the Central Spanish Pyrenees, is the main tributary of the Ésera River, and both are the main contributing rivers to the Barasona reservoir, which supplies water to agricultural lowlands (Fig. 1). The reservoir has suffered from siltation since its construction in 1932 with implications for reservoir management (Navas et al. 1998; Valero-Garcés et al. 1999). A bathymetric survey carried out in 1995 indicated that during 65 years the reservoir had lost about one third of its initial water storage

capacity. During this period, it had been receiving from its contributing drainage catchment (1509 km^2) a specific sediment yield of 350 t km^{-2} $year^{-1}$ (Avendaño-Salas et al. 1997). Previous studies on sediment productions and yields in the Barasona reservoir catchment revealed that the Isábena River catchment, with a surface area of 445 km^2, contributes around 30 % of the sediment yield to the Barasona reservoir (Alatorre et al. 2010; Palazón and Navas 2014) Moreover, the Isábena River catchment, which represents one third of the Barasona catchment, contributes a specific sediment yield of ~460 t km^{-2} $year^{-1}$, indicating the need for targeted erosion management (López-Tarazón et al. 2009, 2012; Alatorre et al. 2010; Palazón and Navas 2014).

The Isábena catchment is characterised by heterogeneous relief, vegetation and soil characteristics. Elevation varies from 450 m a.s.l. at the confluence with the Ésera River to more than 2700 m a.s.l. at the headwater. The headwater of the catchment mostly comprises Triassic and Cretaceous materials, with a predominance of Cretaceous limestones that are partially karstified and have developed deep and narrow gorges. In the intermediate part of the catchment, there are more erodible materials such as Eocene marls that comprise depressions in which badlands are developed. Although badland areas represent <1 % of the catchment, they constitute an important source of sediment (Alatorre and Beguería 2009; Alatorre et al. 2010; López-Tarazón et al. 2012; Palazón and Navas 2014). In the lower part, a relative lowland area, Tertiary detrital sedimentary rocks (clays, sandstones and conglomerates) are predominant (Fig. 2).

Climatically, the catchment belongs to the Mediterranean domain (López-Tarazón et al. 2012). Temperature and precipitation gradients are observed for both north-south and west-east regions according to the relief and climate influences of the Atlantic Ocean and Mediterranean Sea. The topographic heterogeneity of the region partly explains the great spatial variability in annual precipitation, which ranges from 450 mm at the outlet to 1600 mm at the headwater (Verdú et al. 2006a). Mean annual precipitation in the catchment is ~767 mm, with seasonal maxima in spring and autumn (López-Tarazón et al. 2009). Temperatures are mainly dictated by the altitudinal gradient, and the temperature gradient has been estimated to be ~5 °C km^{-1} (e.g., García-Ruiz et al. 2001). As a result, the mean annual temperature ranges from 12.5 °C at the outlet (424 m a.s.l.) to 10°C in the northern part.

From a geomorphologic point of view, active incision/accretion processes have not been observed in the main reach during the last 10 years, so the more contemporary active

geomorphologic processes are mass movements and, especially, water erosion on slopes and badlands (Verdú et al. 2006b).

The hydrologic regime of the study area is transitional nival–pluvial characterised by two maxima (García-Ruiz et al. 2001): the spring period (April–June), due to snowmelt and the late autumn (October–November) due to precipitation. Floods are caused by different mechanisms: late spring–early summer snow melt and heavy rains, summer thunderstorms, and late autumn heavy rains.

In general, the soils of the catchment are stony and alkaline, overlying fractured bedrock with textures from loam to sandy loam. Soils are, in general, shallow (<0.6 m) and well drained with limited average water content and moderate to low structural stability.

The distribution of land uses in the Isábena catchment reflects its intrinsic climatic and topographic variability which also varies from north to south, with grassland and scrubland predominating in the highlands, forests in the ranges and cultivated land in the more gentle southern areas (Fig. 1). The main land uses and land covers in the catchment are forests and pastures that occupy >50 %, followed by scrublands >10% and cultivated land that occupies <20 % (Table 1 and Fig. 2). Climax vegetation of the central and lower parts of the catchment is forests of *Quercus ilex ballota* with *Pinus halepensis* in sunny areas and woodland of *Quercus faginea* in the shady areas. In the northern part, the climax vegetation is forests of *Pinus sylvestris* and *Pinus uncinata*. The main cultivation management practices in the catchment are annual cultivation of rain-fed cereals (barley, wheat and sunflowers), with conservation tillage, in combination with traditional tillage and 'set-aside' (ley) rotations. Important changes in land use occurred during the last 60 years in the Spanish Pyrenean region, resulting in substantial land abandonment that has affected most parts of the agricultural areas, triggering the subsequent process of natural reforestation (García-Ruiz and Valero-Garcés 1998).

2.2 Sample collection

To characterise the signatures of source materials, representative sites were selected by a non-aligned random spatial sampling method as implemented in the open-source R package (spsample function on the sp library). This method generates a random sample while preserving an even spatial distribution of points across the study area. Areas above 2000 m a.s.l. and with >30 % slope gradient were excluded from the sampling.

This exclusion was because these areas comprise massive rock outcrops with very little soil development and vertical slopes, therefore, they do not constitute important sediment sources. In addition, distribution of the representative sites was checked and balanced to align with the percentage distribution of land uses/land covers in the catchment. Samples from the representative sites were taken in areas where there is high potential sediment yield connectivity from hillslope to channel and relative easy access. Part of the upper middle catchment was not sampled due to the above-mentioned exclusion and because its inaccessibility through the gorges and molasses developed in Cretaceous limestones. Soil and subsoil sources and sediment samples were collected and strategically combined in the field to create composite samples representative of the source areas.

A total of 144 individual soil samples, 4 samples per sampling point, were collected by using a cylindrical core 5 cm long and 6 cm of diameter and combined in the field to form 36 composite samples (31 surface and 5 subsoil). The depth of sampling interval was selected because of the stoniness and high surface soil roughness in the study soils. Of the soil samples, 18 were from forest, 9 from agricultural fields and 4 from scrubland. Subsoil source samples comprised three composite samples from badlands in Eocene marls in the intermediate part of the catchment and another two composite samples were from subsoils in eroded areas on marls. Forest source included low-density grazing and these two land uses are referred to as 'forest' in the remainder of the paper. Scrubland sources were separated from the forest source as they were thought to correspond with areas where burning practice to produce pastures for livestock had been common in the beginning of the past century. While some source characterisation is limited in the total number of samples, the spatial integration sampling approach improves the representativeness of resulting data.

Samples of fine reservoir sediments were collected from the delta formed just before the junction of the Isábena River and the Ésera River. Sediment deposition in this delta was thought to be related to periods when the reservoir capacity was full enough to flood this area and stop the inflow of the Isábena River into the Ésera River. These high water levels produce water retention that is likely to create conditions for the deposition of fine sediments similar to that occurring in a delta environment. When the water level decreases, the river incises these fine sediment deposits. Averaged daily level data for the period 2003–2013 of the Barasona reservoir indicate that the period from May to

July is when reservoir levels are highest (Fig. 3), which coincides with spring–snowmelt period. A total of 27 individual samples of surficial fine sediment were collected along the delta following a transect 100 m long from the upper part to the lower part at the junction. Samples were combined in the field to create three composite samples, each made of nine individual samples that were representative of sediment deposited at the upper, middle and low sections of the delta.

In addition, exposed channel bed fine sediments were sampled along the Isábena River as they represent material delivered from the upstream catchment, as intermediate targets, linking the catchment to the reservoir (Fig. 1). Sampling was limited to clearly identifiable depositional zones likely to contain substantial amounts of fine-grained sediment (Horowitz and Stephens 2008) as, in general, the Isábena River flows through blocky or rocky channels. Channel banks are not developed, or they are very local, and therefore, they were not sampled. At each site, a total of six samples were collected along transects of 50 m long and combined to create a composite sample representative of the reach and contributing upstream land use (Table 1).

2.3 Sample analysis

All samples were initially oven-dry to 35 °C, gently disaggregated and sieved to <63 μm to isolate a standardised grain size fraction for source and sediment materials (Smith and Blake 2014). Sample grain size was determined using a laser diffraction particle size analyser (Beckman Coulter LS 13 320, Miami, USA). Prior to grain size analysis, organic matter was eliminated with an H_2O_2 (10 %) digest heated to 80 °C. Samples were disaggregated with sodium hexametaphosphate (40 %), stirred for 2 h and dispersed with an ultrasound for 1 min. Soil organic carbon content was analysed using finely ground subsamples with a dry combustion method using a LECO RC-612 (St. Joseph, USA) multiphase carbon analyser designed to differentiate forms of carbon by oxidation temperature.

Mass-specific magnetic susceptibility (χ) was measured using a Bartington Instruments dual-frequency MS2B sensor (Witney, UK) at low and high frequency to determine frequency dependence of susceptibility (χ_{FD}). Mass-specific magnetic susceptibility at low (χ_{LF}) frequency was expressed as 10^{-8} m^3 kg^{-1}.

The analysis of the total elemental composition was carried out after total acid digestion with HF (48%) in a microwave oven (Navas and Machín 2002). Samples were analysed

for the following 28 elements: Li, K, Na (alkaline), Be, Mg, Ca, Sr (light metals), Cr, Cu, Mn, Fe, Al, Zn, Ni, Co, Cd, Tl, Bi, V, Ti and Pb (heavy metals), B, Sb, As (metalloids), and P, S, Mo and Se. Analyses were performed in triplicate by inductively coupled plasma atomic emission spectrometry with a Perkin Elmer OPTIMA 3200 DV ICP-AES (Waltham, USA) and resulting concentrations expressed in milligrams per kilogram. Those elements returning measurements below the detection limit (Co, Cd and Se) were excluded from the analysis. P was also excluded on the basis of the risk of non-conservative behaviour during downstream transport (Granger et al. 2007).

Radionuclide activity concentrations in the soil samples were measured using a Canberra high-resolution, low background, hyperpure germanium coaxial gamma detector model XtRa GX3019 (Meriden, USA). The detector had a relative efficiency of 50% and a resolution of 1.9 keV (shielded to reduce background) and was calibrated using standard samples that had the same geometry as the measured samples. Subsamples of 50 g were loaded into plastic containers (Navas et al. 2005a, b). Count times over 24 h provided an analytical precision of ~±3–10% at the 95% level of confidence. Activities were expressed as becquerel per kilogram dry soil.

Gamma emissions of ^{238}U, ^{226}Ra, ^{232}Th, ^{40}K, ^{210}Pb and ^{137}Cs (expressed in Bq kg^{-1} air-dry soil) were measured in the bulk soil samples. Considering the appropriate corrections for laboratory background, ^{238}U was determined from the 63-keV line of ^{234}Th, the activity of ^{226}Ra was determined from the 352-keV line of ^{214} Pb (Van Cleef 1994); ^{210}Pb activity was determined from the 47-keV photopeak, ^{40}K from the 1461-keV photopeak; ^{232}Th was estimated using the 911-keV photopeak of ^{228}Ac, and ^{137}Cs activity was determined from the 661.6-keV photopeak. The measured activity concentration of ^{210}Pb is an integration of the 'in situ' geogenic component from decay of ^{226}Ra within the material (Appleby and Oldfield 1992) and the fallout component derived via diffusion of ^{222}Rn. A small part of ^{222}Rn diffuses into the atmosphere providing an input of ^{210}Pb to surface soils which is not in equilibrium with its parent ^{226}Ra. This fallout radionuclide is termed unsupported or excess ^{210}Pb ($^{210}Pb_{ex}$) to distinguish it from the ^{210}Pb fallout component (Gaspar et al. 2013; Mabit et al. 2014). Spectrometric measurements were performed a month after the samples were sealed, which ensured a secular equilibrium between ^{222}Rn and ^{226}Ra. The $^{210}Pb_{ex}$ activities were estimated from the difference between the total ^{210}Pb activity and the ^{226}Ra activity.

2.4 Sediment fingerprinting procedure and statistical analysis for source discrimination

The standard sediment source fingerprinting procedure is based on: (i) statistical analysis of compositional differences to identify a subset of tracer properties that discriminate the sediment sources followed by (ii) the use of mixing models comprising a set of linear equations for each selected tracer properties to estimate by optimization procedures the proportional contributions from each source to downstream sediment (Yu and Oldfield 1989; Collins et al. 1997; Walden et al. 1997; Blake et al. 2012; Smith and Blake 2014). Examination of the range of source and sediment tracer concentrations is an important assessment of the conservative behaviour of each tracer property (Martínez-Carreras 2010a; Wilkinson et al. 2012; Smith and Blake 2014) and tracer properties falling outside the range in source values were removed from subsequent analysis.

Some studies have included tracer dataset pre-treatments to account for differences in particle size, organic matter and conservativeness correction factors (e.g. Collins et al. 1997, Gruszowski et al. 2003, Motha et al. 2003) that could affect the comparison of tracer concentrations between sources and sediments. Recent work (Smith and Blake 2014), however, has shown that the relationships between fingerprint concentrations and correction factors may produce unquantified errors because of their own inherent complexity which makes it difficult to generalise their use. Therefore, it was decided not to incorporate them in this fingerprinting procedure.

The ability of the remaining potential fingerprinting properties to discriminate between the sediment sources was investigated by conducting the nonparametric Kruskal–Wallis *H* test following Collins and Walling (2002). Greater inter-category differences generated larger *H* test statistics. The null hypothesis stating that measurements of fingerprint properties exhibit no significant differences between source categories was rejected as soon as the *H* test statistics reached the critical threshold of 0.05. However, the *H* test does not confirm differences between all possible paired combinations of source categories. Therefore, as suggested by Collins and Walling (2002), stepwise discriminant function analysis (DFA) based on the minimization of Wilks' lambda was used to test the ability of the tracer properties passing the Kruskal–Wallis *H* test to confirm the existence of inter-category contrast and assess the discriminatory power of

those tracer properties, thus determining the optimal group. The DFA selects an optimum composite fingerprint that comprises the minimum number of tracer properties that provide the greatest discrimination between the analysed source materials. The lambda value approaches 0 as the variability within source categories is reduced relative to the variability between categories based on the entry or removal of tracer properties from the analysis.

2.5 Mixing model and optimization

The relative contribution of each potential sediment source was assessed by a mixing model using a new data processing methodology to obtain proportional source contributions for the sediment samples. Similar to other approaches (e.g. Evrard et al. 2011), the procedure seeks to solve the system of linear equations by means of mass balance equations represented by:

$$\sum_{j=1}^{m} a_{i,j} \cdot x_j = b_i \quad (1)$$

While satisfying the following constraints:

$$\sum_{j=1}^{m} x_j = 1 \quad (2)$$

$$0 \leq x_j \leq 1 \quad (3)$$

where b_i is the value of tracer property i ($i = 1$ to n) in the sediment sample, $a_{i,j}$ is the mean concentration of tracer property i in source type j ($j = 1$ to m), x_j is the unknown relative weighting contribution of source type j to the sediment sample, m is the number of potential source types, and n is the number of tracer properties selected in the previous fingerprinting procedure step by the DFA.

The above system of linear equations was solved as an optimization procedure to minimise the objective function or goodness of fit (GOF, based on Motha et al. 2003), defined by:

$$GOF = 1 - \frac{1}{n} \times \left(\sum_{i=1}^{n} \frac{\left| b_i - \sum_{j=1}^{m} x_j a_{i,j} \right|}{\Delta_i} \right) \quad (4)$$

where Δ_i is the range of tracer property i in the dataset and which is used to normalise the tracer properties ranges.

Special attention was given to the optimization stage, wherein a Monte Carlo method was used in solving the above system of linear equations. This robust technique provided the optimal solution after exploring the entire parameter space. For each mixing sample, a large number of iterations were performed generating random weight values under a uniform distribution which satisfied the mixing model constrains. In addition to the optimal solution, the Monte Carlo method generated a range of possible solutions allowing the solution dispersion to be characterised. The generated solutions were ranked by GOF and the mean weighted source contribution and the standard deviation computed from the 100 solutions that best fitted the source fingerprints. This new data processing procedure, written in the C programming language, was designed to evaluate multiple sediment samples simultaneously and, for each sample, deliver the optimal solution and its dispersion (more details in Palazón et al. 2015).

Prior to the mixing model analysis for the catchment, the optimal number of iterations in the Monte Carlo method was evaluated. Different numbers of iterations were tested to evaluate convergence of the solution with the conclusion that 10^6 iterations were adequate to explore the entire parameter space. The number of possible solutions considered to the optimal solution was selected as it corresponds with the 0.01 % of the generated iterations. Random numbers were generated from a user-defined seed allowing the model reproducibility to be tested. In this study, the procedure to solve the mixing model for all sediment samples was repeated with different random seeds to check for consistency in the derived solution.

3 Results

This preliminary fingerprinting approach was based on analysis of contributions from four possible sediment sources: agricultural, forest, subsoil and scrubland. The catchment lowlands were dominated by agriculture, whereas the elevated areas of the northern part of the catchment were largely scrubland. Forest and subsoil sources were dispersed through the whole catchment (Table 1). The scrubland source was separated from forest because some elemental tracer properties (e.g. SOC or ^{137}Cs) were observed to be higher than the equivalent content from the forest source (values in italics, Table 2).

Sediment samples were grouped to assess their optimum composite fingerprint and source contributions in two sediment mixing options: channel bed sediment samples (as

intermediate/secondary mixing samples) and delta sediment samples (as final catchment mixing samples). Sediment samples were grouped based on their locations in the Isábena River and their deposit characteristics. Sampling points represented sediment accumulations from the contributing catchments (Table 3 and Fig. 2).

Grain size analysis of the <2 mm size fraction showed an increasing trend in the content of fine fractions (silt and clay) towards downstream sections of the river (Fig. 4), and the highest clay content was found in the lower reaches, samples CB4 and CB5. For the delta sediments, the content of fine fractions also increased downstream towards the more proximal parts of the delta. Similar fining trends were observed for the <63 μm size fraction of the channel bed and delta sediments (Fig. 4).

3.1 Source fingerprinting discrimination

Prior to undertaking source apportionment procedures, the conservative behaviour of source properties that could potentially be included in the statistically defined optimum fingerprint (Table 2) was considered. $^{210}Pb_{ex}$ was excluded as a sediment source fingerprint because sediments deposited in the delta would have contained both $^{210}Pb_{ex}$ incorporated into the sediment by direct fallout to the sediments and that associated with sediment eroded from the upstream catchment. In addition, TOC, P and grain size fractions were considered non-conservative properties, and therefore, they were also excluded from the analyses following Granger et al. (2007) and Koiter et al. (2013).

The comparison of the range in the 30 remaining tracer properties' concentrations for source and sediment samples resulted in the exclusion of different properties under each mixing scenario (Tables 2 and 3). For the delta sediments, the comparison of the ranges in tracer properties for sources and sediment samples resulted in the exclusion of S. For the channel bed sediments, ^{40}K, Li and Ti were excluded. Most of the tracer properties lay wholly within the range of source materials, indicating that alteration effects may have been relatively small (Walden et al. 1997). The Kruskal–Wallis *H* test resulted in the identification of ^{40}K, ^{137}Cs, ^{226}Ra, ^{232}Th, ^{238}U, LF, FD, Bi, B, Ca, Fe, Li, Mg, Ni, Sr and Ti as optimum tracer properties to discriminate between the four source types at the 5 % confidence level excluding, for the channel bed sediment, those that failed the range test. From those properties that passing the previous steps, the DFA lead to the selection of four tracer properties that formed the optimum fingerprints for both mixing

sediment options: ^{137}Cs, Bi, Ni and Fe. Clear differences were observed between primary properties that were common to both mixing options (Fig. 5).

Comparison of tracer properties selected by the statistical procedures for all target sediments indicated a general coherence in the relative differences between sources for mean and median values (Table 2 and Fig. 5). Based on Wilks´ lambdas of 0.044 and indication that 97.2% of sources were correctly classified, it was considered that good source discrimination was achieved (Table 4). The first two discriminant functions calculated by a DFA from stepwise selected properties for four source classes are depicted in Fig. 6. Source soil samples from forest were found to overlap with the agricultural land group explaining why the DFA did not achieve 100 % of correctly classified sources.

3.2 Mixing model: source apportionments

The unmixing model used all tracer properties that were selected by the DFA as the optimum source fingerprint to solve the mass balance equation. The apportionment source solutions were defined by the mean, standard deviation and the lower GOF of the extracted combinations. The standard deviation of the best combination allowed us to compare and assess the solution dispersion as large values indicate poor source contribution ascription.

The outputs of the mixing model appeared to be stable from different random number seeds supporting the performance of the optimization procedure. In each repeat simple analysis, the solution dispersion associated with the parameter space was within a range of <3% of its mean value (Table 5). Mean proportional contributions from agricultural, forest, scrubland and subsoil sources varied between sediment samples. In addition to proportional source contributions, relative source contributions obtained by dividing the source contribution by the source contribution area were weighted to assess how land use changes relate to source contributions over the longitudinal river reach and the delta (Table 5). The GOF values were all >82 % with the lower values suggesting some scope for refinement of source characterisation. The outputs of the mixing model for the delta sediments presented GOF values of 90 % but also different source apportionments for each sample. The preliminary results using this new data processing methodology allowed us to simultaneously determine the changes in the source contributions from all

parts of the delta deposit. From the upper to the lower part of the delta, there was a decreasing trend in the contribution from agricultural sources and an increase in the contributions from forest, subsoil and scrubland sources. The main apportionment to the upper delta sediment sample D1 comes from agricultural land. For downstream samples (D2 and D3), agricultural source apportionment decreased and contributions from the other sources increased. In relation to relative source contributions, subsoil was a main source for all delta samples.

Channel bed sediment samples presented variable GOF values with the lowest GOF for the headwater sample (sample CB1) and, reassuringly, the lowest predicted model capacity. Assessed source contributions for the channel bed sediments also changed in source apportionment from headwater to downstream samples. For the headwater, the main source contribution was the subsoil that decreased in relative contribution until sample CB3, due to increasing contributions from forest and agricultural sources. Scrubland contributions were not observed downstream of sample CB3. The agricultural source contribution reached a maximum at the intermediate sample CB3 and decreased marginally in the downstream samples closer to the outlet of the catchment. Forest was also predicted to be an important source for sample CB2 (38 %), but limited contributions were predicted for the other channel bed samples. Placing the channel bed sediment apportionment results in a geomorphic context, mixing model results also indicated an important contribution (19 to 89 %) from subsoil sources (eroded areas and badlands) despite its spatial coverage being <4 %. Therefore, apart from samples CB2 and CB3, relative source contribution results supported the importance of subsoil source.

4 Discussion

The four characterised sources for the fingerprinting analysis reflected well the dominant land uses/land covers in the catchment and the likely related erosion processes. Whereas DFA results indicated good source discrimination, there was some overlap with agricultural and forest soil (Fig. 6). This is meaningful in the contest of known catchment history and was most likely due to succession states between former agricultural areas (Brosinsky et al. 2014) that are partly reverting to natural forests after land abandonment (Lasanta and Vicente-Serrano 2012).

Tracer discrimination between sediment sources (Table 2) outlined the importance of the fallout radionuclide ^{137}Cs as an effective sediment source tracer because it accumulated in the surface soil, where it was strongly adsorbed on fine particles, thus distinguishing it from subsurface material (Wallbrink and Murray 1993; He and Walling 1996). Depending on the land use, the soil redistribution processes and the rainfall gradient (Navas et al. 2007), the ^{137}Cs values at the topsoil differ greatly depending on land use and erosion processes as well as geochemical diffusion, bioturbation and elluviation processes (Walling 2003; Mabit et al. 2008). In the present study, differences in ^{137}Cs content between sources and sediment samples reflected well differences between subsoils, which are affected by intense soil erosion processes, and agricultural lands where ^{137}Cs is mixed within the plough layer (Navas et al. 2013; Gaspar and Navas 2013) as well as material from the forest land where the ^{137}Cs peak appeared at or near the soil surface (Wallbrink et al. 1999; Navas et al. 2014). Large differences of Fe content in scrubland, which were doubled those in other land uses, are likely related to the nature of the substrate as scrubland samples are mainly located on Paleozoic slates and quarzites. Higher Ni contents in subsoil samples might reflect a closer link with the mineral components of the substrate in comparison with the other land uses. In the same way, higher Bi contents in subsoil samples, whereas contents in the other land uses are similar, might indicate a simple relationship with the mineral composition of the substrate due to the contribution of parent geological materials (Navas and Machín 2002). Moreover, the highest contents of Ni and Bi in sedimentary rocks are related with argillaceous materials (Kabata-Pendias and Pendias 2001) which coincide with the dominant lithology of the substrate in the subsoil sources.

The magnetic properties were not found to discriminate the sediment sources in this study. In a previous fingerprinting study by Palazón et al. (2014) carried out in the headwater of the Barasona catchment, the low-frequency magnetic susceptibility (LF) was selected for the optimum composite fingerprint to discriminate between soil sources. However, this was not the case in the Isábena catchment likely because its predominant lithology comprises sedimentary rocks with more homogeneous values of magnetic susceptibility, which differed from that of soils on metamorphic and igneous rocks existing in the headwater catchment.

Although the lowest predicted model capacity of the proposed mixing model was observed for CB1 in the headwaters, the high subsoil contribution of the assessed

sediment samples agreed well with the stable characteristics of the dominant local forest source which is mostly covered by alpine pastures in the Isábena headwaters. This is supported by the absence of a cultivated land source in the upper catchments and the observed high connectivity of eroded subsoil in this area. For the lower downstream channel bed samples, the percentage of catchment surface occupied by forest and subsoil slightly decreased in line with an increase in the relative percentage of agricultural land (Table 1). The increase of agricultural inputs to downstream channel bed samples explains the relative decline in the subsoil contribution for lower downstream channel bed sediment samples, i.e. the proportion decreases but mass contribution is likely to remain constant. Sediment load data are required to underpin this. Agricultural source contributions were expected to be greater than assessed for the downstream channel bed sediment samples given the extensive cover of cultivated source area (Table 1). The maximum contribution at sample CB3 is likely to be related to greater connectivity and abundance of farmland slopes at the middle part of the catchment. Low scrubland source contributions assessed for all sediment samples are likely to be due to greater soil stability; this characteristic is provided by high soil organic carbon contents and the effect of dense vegetation cover that limits erosion (Navas et al. 2014), although limited connectivity to the stream cannot be excluded as a factor. Soil stability is supported by the highest ^{137}Cs content in the scrubland source.

The notable agricultural sediment contribution to the upper delta sediment sample, D1, is in accord with the observations regarding lower reach stream sediment above. The decrease in the influence of agricultural sources on the lower part of the delta might be due to reservoir water level dynamics related to climatic and hydrological regime conditions in the catchment. When the upper part of the delta is inundated, conditions in the catchment are more conducive to agricultural soil erosion (i.e. wet periods with high antecedent rainfall conditions). When the reservoir is drawn down during dry periods, the incised landscape is more prone to erosion by discrete events compared to agricultural soils. As noted above, while the present study indicates that the source apportionment approach is performing well within this system, the comparison of source proportions alone can be limiting in the absence of sediment load data. Interpretation of these data in the context of a reservoir sediment budget, based on a detailed survey of sediment deposits, is required to take the analysis further.

Subsoil erosion was shown to be an important source of sediment to the Barasona reservoir. Previous research on sediment yields for the Isábena catchment and the region showed that significant amounts of sediment were generated within the tributary drainage sub-catchment where badlands on marls are developed, just upstream of site CB2 (Fig. 2) (Fargas et al. 1997; López-Tarazón et al. 2009, 2012; Alatorre et al. 2010; Palazón and Navas 2014). Weighting of mixing model results to relative source contributions showed the importance of the subsoil source over the longitudinal river reach and for the delta deposit pointing to its key role in siltation of the Barasona reservoir. Alatorre et al. (2010) simulated sediment yield from land uses using the WATEM/SEDEM model for the Barasona catchment obtaining the highest specific sediment yield from the badland areas. The other simulated land uses yielded less than one order of magnitude than the badlands. Recent fingerprinting work in the Isábena catchment based on spectral fingerprinting (Brosinsky et al. 2014) concluded that spectral fingerprints permit the quantification of subsurface source contributions to artificial mixtures. However, in situ-derived source information was found to be insufficient for real-world apportionment, most likely due to differences in soil moisture conditions and grain size contents in the field.

A number of potential limitations should be taken into account when interpreting the findings of this study. Sampling was only undertaken for a single campaign due to available funding and catchment scale and access, limiting the number of samples, which in turn could restrict the applicability of the results. A greater number of samples are recommended for future research on sediment fingerprinting for the catchment to provide more robust statistical analysis. Even so, the fingerprinting results were in accordance with previous studies in the catchment supporting the representative characteristics of the source samples, which were based on spatially integrated samples. Although the source contributions were in accordance with the upstream distributions of the land uses/land covers, subsoil sources that occupy a relatively small surface area in the catchment are one of the main contributors. Previous studies in the catchment identified subsoil as one of the main sediment source (López-Tarazón et al. 2009; Alatorre et al. 2010; Palazón and Navas 2014). The bed sediment samples enable the source proportions for the sediment sequestered on the river bed at the time of sampling, rather than for all sediments that might have passed through temporary storage at some point during its delivery through the system (Collins et al. 2013). An alternative

approach would be to deploy time-integrating traps (Phillips et al. 2000) for suspended sediment collection, but research has confirmed that bed sediment samples can be used as a surrogate for obtaining representative sediment fingerprinting data (e.g. Horowitz et al. 2012). This situation is especially relevant where long-term channel storage is less likely: channel bed sediment may reflect long-term trends in sediment sources, while the suspended sediment samples represent short-term trends. Further research is needed to understand the role of bed sediment and downstream erosion on sediment dynamics within the Isábena catchment. With respect of bed sediment samples, local factors are likely to also influence the character of stored sediment, such as good mixing conditions at the sampling point and local hydraulic conditions prevailing during the flood recession. As other researchers reported (e.g. Salomons and Förstner 1984; Horowitz 1991) channel bed sediments reflect cumulative additions of chemicals (both sediment-associated and in solution) over time, whereas suspended sediment tend to reflect pulses from specific sources. Results of this first approach could then be usefully compared with the fingerprinting of suspended sediment collected during floods in order to improve the understanding of sediment sources in the Isábena catchment. In mountainous environments, additional factors control the composition of riverbed sediment such as the spatial and temporal rainfall patterns, the sediment source heterogeneity, their connectivity to the river network and their distance from the outlet, the temporal variability of the soil cover by snow and vegetation and the sediment sorting and the abrasion dynamics of the coarser sediment fraction along the river network (Evrard et al. 2011).

5 Conclusions

Reservoir siltation represents an important challenge and its effects can be economically and societally serious in terms of both water and energy security. Therefore, sediment fingerprinting studies are needed to increase knowledge on the origin of fine sediment within the contributing area to improve our understanding of sediment dynamics and provide support for sustainable catchment management. In this study, a new approach to solve fine sediment source fingerprinting mixing equations was applied for a mountain river catchment in the central Spanish Pyrenees that feeds a water supply reservoir. The approach generated uniformly distributed random values which guarantees that all possible solutions were equally tested. It is argued that this method can deliver the

optimal solution in all unmixing cases, thereby allowing a detailed characterisation of the solution and its dispersion.

Agricultural, forest, subsoil and scrubland sources were discriminated though standard statistical analyses, and an optimum composite fingerprinting was defined. The results of the sediment fingerprinting study for the Isábena reservoir catchment based on delta and channel bed sediment samples demonstrated that there were changes in sediment sources between (i) the headwaters and the outlet of the catchment and (ii) the upper and the lower parts of the delta. For the upper part of the delta deposit, agricultural and connected eroding subsoil dominated as main contributing sources, while for the lower part of the delta, subsoil and forest sources were more important, and these were linked to reservoir water levels and the susceptibility of different parts of the landscape to erosion during wet and dry periods.

These results have important implications for the mitigation of reservoir siltation in mountainous catchments as they increase knowledge on the origin of fine sediment that is infilling of the reservoir. Reorganisation of land management systems will benefit from this kind of study which aims at improving sustainability of large infrastructures, such as the Barasona reservoir, while providing a framework to support management plans to assist the regional socio-economy.

Acknowledgements: This research was financially supported by the project CGL2014-52986-R.

References

Acornley RM, Sear DA (1999) Sediment transport and siltation of brown trout (Salmo trutta L.) spawning gravels in chalk streams. Hydrol Process 13:447–458

Alatorre LC, Beguería S (2009) Identification of eroded areas using remote sensing in a badlands landscape on marls in the central Spanish Pyrenees. Catena 76(3):182–190

Alatorre LC, Beguería S, García-Ruiz JM (2010) Regional scale modeling of hillslope sediment delivery: A case study in the Barasona Reservoir watershed (Spain) using WATEM/SEDEM. J Hydrol 391:109–123

Appleby PG, Oldfield F (1992) Application of lead-210 to sedimentation studies. In: Ivanovich M, Harman RS (eds) Uranium-series disequilibrium: application to

earth, marine and environmental sciences, edited by: Clarendon, Oxford, pp731–738.

Avendaño-Salas C, Sanz-Montero E, Cobo-Rayán R, Gómez-Montaña JL (1997) Sediment yield at Spanish reservoirs and its relationship with the drainage basin area. In: Proceedings of the 19th symposium of large dams. ICOLD (International Committee on Large Dams), Florence, Italy, pp 863–874

Blake WH, Ficken KJ, Taylor P, Russell MA, Walling DE (2012) Tracing crop-specific sediment sources in agricultural catchments. Geomorphology 139–140:322–329

Brosinsky A, Foerster S, Segl K, Kaufmann K (2014) Spectral fingerprinting: sediment source discrimination and contribution modelling of artificial mixtures based on VNIR-SWIR spectral properties. J Soil Sediment. 14:1949–1964

Collins A, Walling D (2002) Selecting fingerprint properties for discriminating potential suspended sediment sources in river basins. J Hydrol 261:218–244

Collins AL, Walling DE (2004) Documenting catchment suspended sediment sources: problems, approaches and prospects. Prog Phys Geog 28:159–196

Collins AL, Walling DE, Leeks GJ (1997) Source type ascription for fluvial suspended sediment based on a quantitative composite fingerprinting technique. Catena 29:1–27

Collins AL, Walling DE, Stroud RW, Robson M, Peet LM (2010a) Assessing damaged road verges as a suspended sediment source in the Hampshire Avon catchment, southern United Kingdom. Hydrol Process 24(9):1106–1122

Collins AL, Walling DE, Webb L, King P (2010b) Apportioning catchment scale sediment sources using a modified composite fingerprinting technique incorporating property weighting and prior information. Geoderma 155:249–261

Collins AL, Zhang YS, Duethmann D, Walling DE, Black KS (2013) Using a novel tracing-tracking framework to source fine-grained sediment loss to watercourses at sub-catchment scale. Hydrol Process 27:959–974

Davis CM, Fox JF (2009) Sediment fingerprinting: review of the method and future improvements for allocating nonpoint source pollution. J Environ Eng 135:490–504

Devereux OH, Prestegaard KL, Needelman BA, Gellis AC (2010) Suspended-sediment sources in an urban watershed, Northeast Branch Anacostia River, Maryland. Hydrol Process 24:1391–1403

Dirszowsky RW (2004) Bed sediment sources andmixing in the glacierized upper Fraser River watershed, east-central British Columbia. Earth Surf Process Landf 29:533–552

Evans R, Boardman J (1994) Assessment of water erosion in farmers' fields in the UK. In: Rickson RJ (ed) Conserving soil resources: European perspectives. CAB International, Wallingford, pp 13–24

Evrard O, Navratil O, Ayrault S, Ahmadi M, Némery J, Legout C, Lefèvre I, Poirel A, Bonté P, Esteves M (2011) Combining suspended sediment monitoring and fingerprinting to determine the spatial origin of fine sediment in a mountainous river catchment. Earth Surf Proc Land 36:1072–1089

Fargas D, Martínez Casasnovas JA, Poch R (1997) Identification of Critical Sediment Source Areas at Regional Level. Phys Chem Earth 22:355–359

García-Ruiz JM, Valero-Garcés BL (1998) Historical geomorphic processes and human activities in the Central Spanish Pyrenees. Mt Res Dev 18:309–320

García-Ruiz JM, Beguería S, López-Moreno JI, Lorente A, Seeger M (2001) Los Recursos hídricos superficiales del Pirineo aragonés y su evolución reciente. Geoforma Ediciones, Logroño, Spain

Gaspar L, Navas A (2013) Vertical and lateral distributions of ^{137}Cs in cultivated and uncultivated soils on Mediterranean hillslopes. Geoderma 207–208:131–143

Gaspar L, Navas A, Walling DE, Machín J, Gómez Arozamena, J (2013) Using ^{137}Cs and ^{210}Pbex to assess soil redistribution on slopes at different temporal scales. Catena 102:46–54

Gibbs MM (2008) Identifying source soils in contemporary estuarine sediments: A new compound-specific isotope method. Estuar Coast 31:344–359

Granger SJ, Bol R, Butler PJ, Haygarth PM, Naden P, Old G, Owens PN, Smith BPG (2007) Processes affecting transfer of sediment and colloids, with associated phosphorus, from intensively farmed grasslands: tracing sediment and organic matter. Hydrol Process 21:417–422

Grimshaw DL, Lewin J (1980) Source identification for suspended sediments. J Hydrol 47:151–162

Gruszowski KE, Foster IDL, Lees A (2003) Sediment sources and transport pathways in a rural catchment, Herefordshire, UK. Hydrol Process 17:2664–2681

Haddadchi A, Olley J, Laceby P (2014) Accuracy of mixing models in predicting sediment source contributions. Sci Total Environ 497:139-152

Hancock GJ, Revill AT (2013) Erosion source discrimination in a rural Australian catchment using compound-specific isotope analysis (CSIA). Hydrol Process 27:923–932

He Q, Walling DE (1996) Interpreting particle size effects in the adsorption of ^{137}Cs and unsupported ^{210}Pb by mineral soils and sediments. J Environ Radioactiv 30:117–137

Horowitz AJ (1991) A primer on sediment-trace element chemistry. Sediment-trace element chemistry 2nd edn. Lewis, Chelsea, p 136

Horowitz AJ, Stephens VC (2008) The effects of land use on fluvial sediment chemistry for the conterminous US—results from the first cycle of the NAWQA program: trace and major elements, phosphorus, carbon, and sulfur. Sci Total Environ 400:290–314

Horowitz AJ, Stephens VC, Elrick KA, Smith JA (2012) Annual fluxes of sediment-associated trace/major elements, carbon, nutrients and sulphur from US coastal rivers. In: Collins AL, Golosov V, Horowitz AJ, Lu X, Stone M, Walling DE, Zhang X (eds) Erosion and sediment yields in the changing environment, IAHS Publ 356, IAHS, Wallingford, p 39–48

Hughes AO, Olley JM, Croke JC, McKergow LA (2009) Sediment source changes over the last 250 years in a dry-tropical catchment, central Queensland, Australia. Geomorphology 104:262–275

Kabata-Pendias A, Pendias H (2001) Trace elements in soils and plants. CRC, Boca Raton, p 315

Koiter AJ, Owens PN, Petticrew EL, Lobb DA (2013) The behavioural characteristics of sediment properties and their implications for sediment fingerprinting as an approach for identifying sediment sources in river basins. Earth-Sci Rev 125:24–42

Krein A, Petticrew EL, Udelhoven T (2003) The use of fine sediment fractal dimensions and color to determine sediment sources in a small watershed. Catena 53:165–179

Lal R (1998) Soil erosion impact on agronomic productivity and environment quality. CRC Crit Rev Plant Sci 17:319–464

Lasanta T, Vicente-Serrano SM (2012) Complex land cover change processes in semiarid Mediterranean regions: an approach using Landsat images in northeast Spain. Remote Sens Environ 124:1–14

López-Tarazón JA, Batalla RJ, Vericat D, Francke T (2009) Suspended sediment transport in a highly erodible catchment: The River Isábena (Southern Pyrenees) Geomorphology 109:210–221

López-Tarazón JA, Batalla RJ, Vericat D, Francke T (2012) The sediment budget of a highly dynamic mesoscale catchment: the River Isábena. Geomorphology 138:15–28

Mabit L, Benmansour M, Walling DE (2008) Comparative advantages and limitations of the fallout radionuclides ^{137}Cs, ^{210}Pbex and ^{7}Be for assessing soil erosion and sedimentation. J Environ Radioact 99:1799–1807

Mabit L, Benmansour M, Abril JM, Walling DE, Meusburger K, Iurian AR, Bernard C, Tarján S, Owens PN, Blake WH, Alewell C (2014) Fallout ^{210}Pb as a soil and sediment tracer in catchment sediment budget investigations: a review. Earth-Sci Rev 138:335–351

Mano V, Nemery J, Belleudy P, Poirel A (2009) Assessment of suspended sediment transport in four Alpine watersheds (France): influence of the climatic regime. Hydrol Process 23:777–792

Martínez-Carreras N, Udelhoven T, Krein A, Gallart F, Iffly JF, Ziebel J, Hoffmann L, Pfister L, Walling DE (2010a) The use of sediment colour measured by diffuse reflectance spectrometry to determine sediment sources: application to the Attert River catchment (Luxembourg). J Hydrol 382:49–63

Martínez-Carreras N, Krein A, Udelhoven T, Gallart F, Iffly JF, Hoffman L, Pfister L,Walling DE (2010b) A rapid spectral-reflectance based fingerprinting approach for documenting suspended sediment sources during storm runoff events. J Soils Sediments 10:400–413

Martínez-Carreras N, Krein A, Gallart F, Iffly JF, Pfister L, Hoffmann L, Owens PN (2010c) Assessment of different colour parameters for discriminating potential suspended sediment sources and provenance: a multi-scale study in Luxembourg. Geomorphology 118:118–129

Meybeck M, Laroche L, Dürr HH, Syvitski JPM (2003) Global variability of daily total suspended solids and their fluxes in rivers. Glob Planet Chang 39:65–93

Minella JPG, Walling DE, Merten GH (2008) Combining sediment source tracing techniques with traditional monitoring to assess the impact of improved land management on catchment sediment yields. J Hydrol 348:546–563

Mizugaki S, Onda Y, Fukuyama T, Koga S, Asai H, Hiramatsu S (2008) Estimation of suspended sediment sources using ^{137}Cs and ^{210}Pbex in unmanaged Japanese cypress plantation watersheds in southern Japan. Hydrol Process 22:4519–4531

Molino B, Viparelli R, De Vincenzo A (2007) Effects of river network works and soil conservation measures on reservoir siltation. Int J Sediment Res 22:273–281

Motha JA, Wallbrink PJ, Hairsine PB, Grayson RB (2003) Determining the sources of suspended sediment in a forested catchment in southeastern Australia. Water Resour Res 39:1059

Mukundan R, Radcliffe DE, Ritchie JC, Risse LM, McKinley RA (2010) Sediment fingerprinting to determine the source of suspended sediment in a southern Piedmont stream. J Environ Qual 39:1328–1337

Mukundan R, Walling DE, Gellis AC, Slattery C, Radcliffe DE (2012) Sediment source fingerprinting: transforming froma research tool to a management tool. J Am Water Resour Assoc 48:1241–1257

Navas A, Machín J (2002) Spatial distribution of heavy metals and arsenic in soils of Aragón (northeast Spain): controlling factors and environmental implications. Appl Geochem 17:961–973

Navas A, Valero B, Machín J, Walling D (1998) Sediments of Joaquin Costa reservoir and the history of its deposit [Los sedimentos del embalse de Joaquín Costa y la historia de su depósito]. Limnetica 14:93–102

Navas A, Valero-Garcés BL, Machín J (2004) An approach to integrated assessement of reservoir siltation: the Joaquín Costa reservoir as case study. Hydrol Earth System Sci 8:1193–1199

Navas A, Soto J, López-Martínez J (2005a) Radionuclides in soils of Byers Peninsula, South Shetland Islands, Western Antarctica. Appl Radiat Isot 62:809–816

Navas A, Machín J, Soto J (2005b) Mobility of natural radionuclides and selected major and trace elements along a soil toposequence in the central Spanish Pyrenees. Soil Sci 170:743–757

Navas A, Walling DE, Quine T, Machín J, Soto J, Domenech S, López-Vicente M (2007) Variability in ^{137}Cs inventories and potential climatic and lithological controls in central Ebro valley, Spain. J Radioanal Nucl Chem 274:331–339

Navas A, Valero-Garcés BL, Gaspar L, Palazón L, Machín J (2011) Radionuclides and stable elements in the sediments of the Yesa Reservoir, Central Spanish Pyrenees. J Soils Sediments 11:1082–1098

Navas A, López-Vicente M, Gaspar L, Machín J (2013) Assessing soil redistribution in a complex karst catchment using fallout ^{137}Cs and GIS. Geomorphology 196:231–241

Navas A, López-Vicente M, Gaspar L, Palazón L, Quijano L (2014) Establishing a tracer based sediment budget to preserve wetlands in Mediterranean mountain agroecosystems (NE Spain). Sci Total Environ 496:132–143

Navratil O, Evrard O, Esteves M, Legout C, Ayrault S, Némery J, Mate-Marin A, Ahmadi M, Lefèvre I, Poirel A, Bonté P (2012) Temporal variability of suspended sediment sources in an alpine catchment combining river/rainfall monitoring and sediment fingerprinting. Earth Surf Proc Land 37:828–846

Olley JM, Caitcheon G (2000) Major element chemistry of sediments from the Darling–Barwon river and its tributaries: implications for sediment and phosphorus sources. Hydrol Process 14:1159–1175

Owens PN, Walling DE, Leeks GJL (2000) Tracing fluvial suspended sediment sources in the catchment of the River Tweed, Scotland, using composite fingerprints and a numerical mixing model. In: Foster, IDL (ed) Tracers in geomorphology. Wiley, Chichester, pp 291–308

Owens PN, Blake WH, Giles TR, Williams ND (2012) Determining the effects of wildfire on sediment sources using 137Cs and unsupported 210Pb: The role of landscape disturbances and driving forces. J Soils Sediments 12:982–994

Palazón L, Navas A (2014) Modeling sediment sources and yields in a Pyrenean catchment draining to a large reservoir (Ésera River, Ebro Basin). J Soil Sediment 14:1612–1625

Palazón L, Gaspar L, Latorre B, Blake W, Navas A (2014) Evaluating the importance of surface soil contributions to reservoir sediment in alpine environments: a combined modelling and fingerprinting approach in the Posets-Maladeta Natural Park. Solid Earth 5:963–978

Palazón L, Latorre B, Gaspar L, Blake WH, Smith HG, Navas A (2015) Comparing catchment sediment fingerprinting procedures using an auto-evaluation approach with virtual mixtures. Sci Total Environ http://dx.doi.org/10.1016/j.scitotenv.2015.05.003

Peart MR, Walling DE (1986) Fingerprinting sediment sources: the example of a drainage basin in Devon, UK. In: Hadley RF (ed). Drainage basin sediment delivery. IAHS Publ 159, IAHS, Wallingford, pp 41–55

Phillips JM, Russell MA, Walling DE (2000) Time-integrated sampling of fluvial suspended sediment: a simple methodology for small catchments. Hydrol Process 14:2589–2602

Salomons W, Förstner U (1984) Metals in the hydrocycle. Springer, Berlin, pp 349

Schuller P, Walling DE, Iroumé A, Quilodrán C, Castillo A, Navas A (2013) Using ^{137}Cs and $^{210}Pb_{ex}$ and other sediment source fingerprints to document suspended sediment sources in small forested catchments in south-central Chile. J Environ Rad 124:147–159

Smith HG, Blake WH (2014) Sediment fingerprinting in agricultural catchments: A critical re-examination of source discrimination and data corrections. Geomorphology 204:177–191

Valero-Garcés BL, Navas A, Machín J, Walling D (1999) Sediment sources and siltation in mountain reservoirs: a case study from the Central Spanish Pyrenees. Geomorphology 28:23–41

Van Cleef DJ (1994) Determination of ^{226}Ra in soil using ^{214}Pb and ^{214}Bi inmediately after sampling. Health Phys 67:288–289

Verdú JM, Batalla RJ, Martínez-Casasnovas JA (2006a) Estudio hidrológico de la cuenca del río Isábena (Cuenca del Ebro). I: Variabilidad de la precipitación. Ingeniería del Agua 13:321–330

Verdú JM, Batalla RJ, Martínez-Casasnovas JA (2006b) Estudio hidrológico de la cuenca del río Isábena (Cuenca del Ebro). II: Respuesta hidrológica. Ingeniería del Agua 13:331–343

Walden J, Slattery MC, Burt TP (1997) Use of mineral magnetic measurements to fingerprint suspended sediment sources: approaches and techniques for data analysis. J Hydrol 202:353–372

Wallbrink PJ, Murray AS (1993) Use of fallout radionuclides as indicators of erosion processes. Hydrol Process 7:297–304

Wallbrink PJ, Murray AS, Olley JM (1999) Relating suspended sediment to its original depth using fallout radionuclides. Soil Sci Soc Am J 63: 369–378

Walling DE (2003) Using environmental radionuclides as tracers in sediment budget investigations. In: Bogen J, Fergus T, Walling DE (eds) Erosion and sediment transport measurement in rivers: technological and methodological advances. IAHS Publ 283, IAHS, Wallingford, pp 57–78

Walling DE (2005) Tracing suspended sediment sources in catchments and river systems. Sci Total Environ 344:159–184

Walling DE (2013) The evolution of sediment source fingerprinting investigations in fluvial systems. J Soils Sediments 13:1658–1675

Walling DE, Collins AL, McMellin GK (2003) A reconnaissance survey of the source of interstitial fine sediment recovered from salmonid spawning gravels in England and Wales. Hydrobiologia 497:91–108

Waters TF (1995) Sediment in streams: sources, biological effects and control. American Fisheries Society, Bethesda,

Wilkinson SN, Hancock GJ, Bartley R, Hawdon AA, Keen RJ (2012) Using sediment tracing to assess processes and spatial patterns of erosion in grazed rangelands, Burdekin River basin, Australia. Agric Ecosyst Environ 180:90–102

Wischmeier WH, Smith DD (1978) Predicting rainfall erosion losses. In: Agricultural handbook 537. USDA. Agricultural Research Service, Washington

Wood PJ, Armitage PD (1997) Biological effects of fine sediment in the lotic environment. Environ Manag 21:203–217

Wood PJ, Armitage PD (1999) Sediment deposition in a small lowland stream: management implications. Regul Rivers 15:199–210

Yu L, Oldfield F (1989) A multivariate mixing model for identifying sediment source from magnetic measurements. Quat Res 32:168–181

Table 1.- Distribution (%) of sources and rock outcrops in the contributing areas for the sampling points of the channel beds (CB1–CB5) and delta sediments in the Isábena catchment.

	CB1	CB2	CB3	CB4	CB5	Delta
Forest	75	72	72	71	70	68
Agricultural	0	1	5	12	15	17
Subsoil	4	2	3	2	2	2
Scrubland	10	21	16	11	10	9
Rock outcrops	11	4	4	4	3	3

Table 2.-Statistics of the tracer properties for the potential sediment sources (units: textural classes: %; radionuclide: Bq kg^{-1}; low frequency mass specific magnetic susceptibility 10^{-8} m^3 kg^{-1} and magnetic susceptibility frequency dependence %; total elemental composition: mg kg^{-1}).

	Agricultural		n=9			Forest		n=18		
	m[a]	mn[b]	sd[c]	min[d]	max[e]	m[a]	mn[b]	sd[c]	min[d]	max[e]
Clay	18.1	17.9	3.7	12.8	24.8	15.6	16.3	2.8	10.3	19.1
Silt	74.5	74.2	2.9	70.8	79.0	72.2	72.0	3.6	66.2	78.1
Sand	7.5	7.3	2.4	4.4	13.0	12.2	12.4	4.1	6.6	23.3
^{137}Cs	6.5	6.8	2.8	2.2	10.2	*39.2*	*36.9*	24.1	3.1	81.5
^{40}K	529.4	534.0	116.6	348.0	724.0	487.3	503.5	79.7	362.0	638.0
^{238}U	44.6	41.7	10.2	31.3	59.3	48.4	49.1	7.6	30.6	60.2
^{232}Th	30.9	31.8	7.3	18.7	38.9	34.7	35.2	8.0	17.7	45.8
^{226}Ra	28.1	27.0	5.8	19.1	38.7	28.5	28.4	5.0	19.0	40.6
SOC[f]	1.4	1.5	0.5	0.5	2.1	*4.8*	*3.4*	4.0	0.8	14.7
LF[g]	16.3	12.6	10.8	5.9	40.6	50.0	14.2	84.0	4.1	347.4
FD[h]	7.9	8.2	2.3	4.5	11.4	7.0	7.3	2.3	2.3	10.2
Ca	96,853.3	79,250.0	47,946.4	51,580.0	17,0700.0	73,547.0	77,395.0	34,427.3	6164.0	153,500.0
Al	31,657.8	30,460.0	8344.2	16,880.0	46,140.0	35,478.2	34,500.0	12,170.7	9648.0	61,920.0
Fe	18,630.1	19,020.0	4812.5	7801.0	25,580.0	22,980.8	20,220.0	9861.9	6094.0	43,890.0
K	12,117.6	12,300.0	3637.6	8333.0	18,470.0	11,568.9	11,715.0	2230.1	7079.0	14,680.0
B	4712.2	4870.0	1354.7	2810.0	6740.0	3271.1	3240.0	1297.0	489.4	5290.0
Na	4236.2	3795.0	1541.5	2432.0	6444.0	3783.9	3598.0	1151.4	2353.0	6525.0
Mg	3672.4	3420.0	771.1	2604.0	4951.0	3431.3	3354.5	676.3	2561.0	5422.0
Ti	3084.4	3070.0	571.6	1830.0	3930.0	3442.8	3215.0	902.5	2110.0	5170.0
S	844.8	804.7	178.9	656.7	1134.0	937.1	918.6	143.7	658.5	1190.0
P	574.6	570.5	138.7	356.8	791.4	498.9	419.9	266.2	292.7	1317.0
Mn	338.3	339.3	51.8	247.9	400.5	405.6	303.3	290.3	184.4	1176.0
Sr	167.4	174.6	55.4	80.3	260.8	214.0	203.0	121.0	39.9	450.5
Zn	136.1	67.7	116.7	49.2	338.3	65.9	47.2	46.6	30.2	216.7
V	67.6	67.7	19.2	36.7	110.1	76.2	75.7	21.1	30.3	114.0
Cr	44.5	46.7	11.3	21.3	57.8	55.1	50.2	17.8	20.3	86.2
Li	40.3	40.9	7.1	27.7	48.3	40.5	38.4	9.6	20.4	56.6
Ni	37.4	37.2	4.6	32.4	45.9	32.5	32.4	5.2	24.6	46.1
As	31.0	6.8	39.0	3.0	95.8	8.3	4.4	12.5	1.7	55.6
Tl	25.0	25.5	4.6	14.4	29.2	26.9	25.6	6.9	15.2	43.8
Pb	23.3	23.4	5.1	15.4	32.0	26.9	27.4	8.6	13.9	48.0
Bi	20.6	20.4	2.3	16.8	25.4	20.7	21.0	3.8	13.6	26.6
Cu	15.0	14.4	3.1	8.8	19.9	12.9	11.5	5.5	5.9	26.7
Se	5.0	6.0	3.1	1.0	9.1	2.2	1.2	2.5	0.0	10.1
Sb	4.6	2.7	4.8	0.6	12.7	2.6	1.8	2.2	0.0	8.7
Be	1.2	1.2	0.6	0.0	2.2	1.2	1.2	0.5	0.0	1.9

[a] mean; [b] median; [c] standard deviation; [d] minimum; [e] maximum; [f] soil organic carbon; [g] low frequency mass specific magnetic susceptibility; [h] magnetic susceptibility frequency dependence

Table 2.- (continued)

	Scrubland		n=4			Subsoil		n=5		
	m[a]	mn[b]	sd[c]	min[d]	max[e]	m[a]	mn[b]	sd[c]	min[d]	max[e]
Clay	14.2	14.1	1.1	13.0	15.5	15.0	13.9	4.1	10.5	19.7
Silt	69.1	70.9	4.5	62.5	72.0	74.3	74.8	1.7	72.2	75.9
Sand	16.8	15.6	3.6	13.8	22.0	10.7	12.2	3.7	5.5	13.9
^{137}Cs	*150.0*	*146.0*	37.0	110.0	710.0	0.4	0.0	0.6	0.0	1.3
^{40}K	635.3	633.5	63.4	564.0	198.0	608.2	655.0	128.6	464.0	759.0
^{238}U	61.7	61.5	3.3	58.0	38.8	44.8	44.6	4.8	37.3	49.8
^{232}Th	60.7	60.5	13.2	48.6	73.4	31.9	31.6	9.2	23.2	45.1
^{226}Ra	35.1	35.7	3.8	30.3	65.9	36.3	35.0	8.2	26.4	44.8
SOC[f]	*13.4*	*12.9*	1.9	11.7	16.1	0.5	0.5	0.2	0.4	0.9
LF[g]	54.1	54.0	23.2	32.9	75.4	6.0	5.9	1.5	4.6	8.0
FD[h]	10.1	10.2	0.7	9.1	10.9	4.8	2.9	5.0	1.3	13.6
Ca	3128.3	2371.0	2497.5	1040.0	6731.0	114,996.0	102,100.0	32,366.5	79,350.0	153,600.0
Al	42,785.0	45,685.0	7285.2	32,140.0	47,630.0	40,434.0	26,820.0	34,441.9	20,140.0	101,300.0
Fe	36,087.5	36,220.0	4858.4	31,380.0	40,530.0	18,132.0	17,980.0	937.6	17,030.0	19,300.0
K	13,270.0	12,815.0	1975.7	11,450.0	16,000.0	16,076.0	13,720.0	5726.6	10,500.0	25,230.0
B	1107.8	1310.0	460.5	421.0	1390.0	3138.0	3840.0	1455.8	1350.0	4420.0
Na	5238.0	5695.5	1526.9	3026.0	6535.0	4957.2	4277.0	1510.1	3853.0	7577.0
Mg	1964.1	1573.6	1355.3	919.1	3790.0	6432.4	6620.0	3205.0	2532.0	9950.0
Ti	4415.0	4610.0	1002.8	3040.0	5400.0	2504.0	2460.0	573.7	1880.0	3140.0
S	645.4	642.8	74.5	559.6	736.4	1255.9	1164.0	377.0	929.5	1907.0
P	798.6	697.6	336.8	513.3	1286.0	527.1	493.0	60.5	475.9	595.1
Mn	569.7	565.7	202.3	326.0	821.3	400.4	341.1	126.0	296.9	610.5
Sr	43.2	40.1	17.4	27.4	65.0	496.1	272.9	350.3	217.0	1010.0
Zn	84.3	76.5	30.6	56.4	127.9	61.5	57.3	11.8	50.5	81.5
V	87.1	90.8	42.8	33.8	132.8	107.0	95.8	36.2	72.4	166.9
Cr	70.1	71.1	25.8	38.1	100.0	76.2	55.5	43.8	44.6	152.2
Li	56.9	50.1	27.2	33.3	94.3	66.8	56.9	20.4	49.3	99.4
Ni	22.8	23.4	7.6	13.2	31.4	46.6	37.8	14.9	34.8	69.8
As	14.1	2.3	25.2	0.0	51.8	4.9	5.4	2.6	1.0	7.8
Tl	29.2	28.4	5.5	23.6	36.5	38.5	32.8	16.3	21.6	59.8
Pb	36.9	36.1	8.4	29.4	45.8	25.6	23.9	7.5	17.7	38.1
Bi	22.4	21.8	3.0	20.0	26.3	30.3	24.9	9.3	22.7	44.4
Cu	14.9	14.7	2.4	12.5	17.9	14.9	15.5	1.8	11.8	16.6
Se	0.5	0.0	0.9	0.0	1.9	2.7	2.1	1.9	1.5	6.0
Sb	4.7	4.8	0.8	3.7	5.5	1.5	1.3	1.5	0.0	4.0
Be	1.7	1.7	0.5	1.2	2.3	1.8	1.8	0.7	1.0	2.9

[a] mean; [b] median; [c] standard deviation; [d] minimum; [e] maximum; [f] soil organic carbon; [g] low frequency mass specific magnetic susceptibility; [h] magnetic susceptibility frequency dependence

Table 3.- Values of the tracer properties for the delta (D1–D3) and channel bed sediment samples (CB1–CB5) (units: textural classes: %; radionuclide: Bq kg^{-1}; low frequency mass specific magnetic susceptibility 10^{-8} m^3 kg^{-1} and magnetic susceptibility frequency dependence %; total elemental composition: mg kg^{-1}).

	Delta samples			Channel bed samples				
	D1	D2	D3	CB1	CB2	CB3	CB4	CB5
Clay	9.4	15.9	19.7	7.9	15.2	8.4	8.4	9.3
Silt	77.2	67.3	76.6	64.6	78.6	83.6	77.8	80.1
Sand	13.4	16.9	3.7	27.5	13.5	8.0	13.8	10.6
^{40}K	461.0	556.0	586.0	851.0	387.0	423.0	372.0	403.0
^{137}Cs	0.0	0.0	1.7	11.6	0.0	0.0	0.0	0.0
^{226}Ra	27.9	27.6	27.7	41.6	27.0	29.1	29.9	30.2
^{232}Th	30.9	37.3	34.8	56.9	31.5	31.5	30.9	36.0
^{238}U	43.6	51.9	50.2	57.2	64.7	31.3	38.7	41.2
SOC[a]	0.3	0.4	0.4	1.5	0.2	0.2	0.2	0.2
LF[b]	14.2	9.9	12.7	22.5	4.7	5.1	4.6	4.6
FD[c]	4.9	7.1	1.6	7.6	4.3	9.8	6.5	4.4
Ca	140,800.0	116,300.0	115,900.0	18,840.0	129,200.0	114,900.0	117,100.0	118,300.0
Al	29,190.0	28,130.0	27,540.0	46,680.0	29,560.0	25,920.0	23,670.0	24,130.0
Fe	19,800.0	20,440.0	21,850.0	37,650.0	20,300.0	18,680.0	16,740.0	16,430.0
K	10,500.0	11,800.0	12,430.0	15,920.0	9781.0	9388.0	9287.0	10,740.0
Na	4259.0	3408.0	4672.0	4246.0	6410.0	4538.0	5468.0	4242.0
Mg	4064.0	3367.0	4006.0	1975.0	4418.0	3071.0	4206.0	4106.0
B	3910.0	3690.0	3950.0	720.2	3930.0	3510.0	4800.0	4780.0
Ti	2900.0	2730.0	2820.0	5700.0	3460.0	3150.0	3120.0	3030.0
S	2661.0	2010.0	2094.0	659.2	3420.0	3405.0	3409.0	2824.0
P	441.4	402.6	445.1	761.6	293.5	306.5	269.5	289.0
Sr	413.2	395.8	428.0	82.4	399.4	366.0	377.1	357.2
Mn	282.1	239.9	273.8	366.7	239.0	246.7	275.8	288.7
V	61.8	75.0	82.6	118.5	53.6	55.5	55.7	59.5
Zn	40.6	40.8	45.4	70.0	33.9	38.1	37.1	40.1
Cr	40.1	48.3	55.6	78.3	34.7	34.7	27.3	30.0
Li	38.1	47.9	48.8	105.0	36.8	35.4	35.6	37.7
Tl	29.3	26.1	30.2	32.4	29.1	23.6	27.6	28.9
Bi	23.7	22.9	25.7	29.8	24.7	22.6	24.5	24.3
Ni	21.5	21.4	24.2	32.0	21.0	21.7	22.1	22.7
Pb	19.8	18.9	19.6	28.2	19.3	17.8	20.6	21.0
Cu	10.0	8.9	11.0	20.9	7.6	8.5	9.0	9.9
As	8.2	4.8	5.6	5.9	11.7	8.9	9.6	8.3
Sb	1.5	1.5	1.3	4.4	1.2	1.4	1.0	1.4
Se	1.4	2.2	2.4	1.8	1.2	1.5	1.2	1.0
Be	0.9	1.3	1.2	2.2	0.9	0.8	0.8	0.9

[a] soil organic carbon; [b] low frequency mass specific magnetic susceptibility; [c] magnetic susceptibility frequency dependence

Table 4.- Results of the stepwise discriminant function analysis to identify the optimum composite fingerprint.

Fingerprint property added	Wilks' lambda
^{137}Cs	0.175
Bi	0.100
Ni	0.070
Fe	0.044

Table 5.- Mean percentages of GOF, source contributions (standard deviations in parentheses) and relative source contributions (RSC) from the multivariate mixing model for agricultural, forest, subsoil and scrubland sources to the channel beds (CB1–CB5) and delta sediments (D1–D3).

	GOF	Agricultural		Forest		Subsoil		Scrubland	
Channel beds	%	%	RSC	%	RSC	%	RSC	%	RSC
CB1	82	1(1)		2(1)	0.15	89(1)	138.87	8(1)	4.58
CB2	90	20 (3)	19.56	38(3)	0.28	41(0)	9.02	1(1)	0.02
CB3	91	78 (2)	5.73	2(1)	0.01	19(1)	2.75	0(0)	0.00
CB4	90	59 (2)	1.33	1(1)	0.00	39(2)	5.09	0(0)	0.00
CB5	90	61(2)	0.93	2(1)	0.01	37(2)	3.96	0(0)	0.00
Delta									
D1	90	43 (3)	0.58	25(3)	0.08	31(0)	3.08	1(1)	0.02
D2	90	37 (2)	0.50	39(3)	0.13	23(0)	2.29	1(1)	0.02
D3	90	1 (1)	0.01	44(2)	0.15	51(1)	5.07	4(3)	0.10

Figures:

Fig. 1 Location of the Isábena catchment in the Iberia Peninsula, digital elevation model (DEM), distribution of land uses/land covers and sampling points

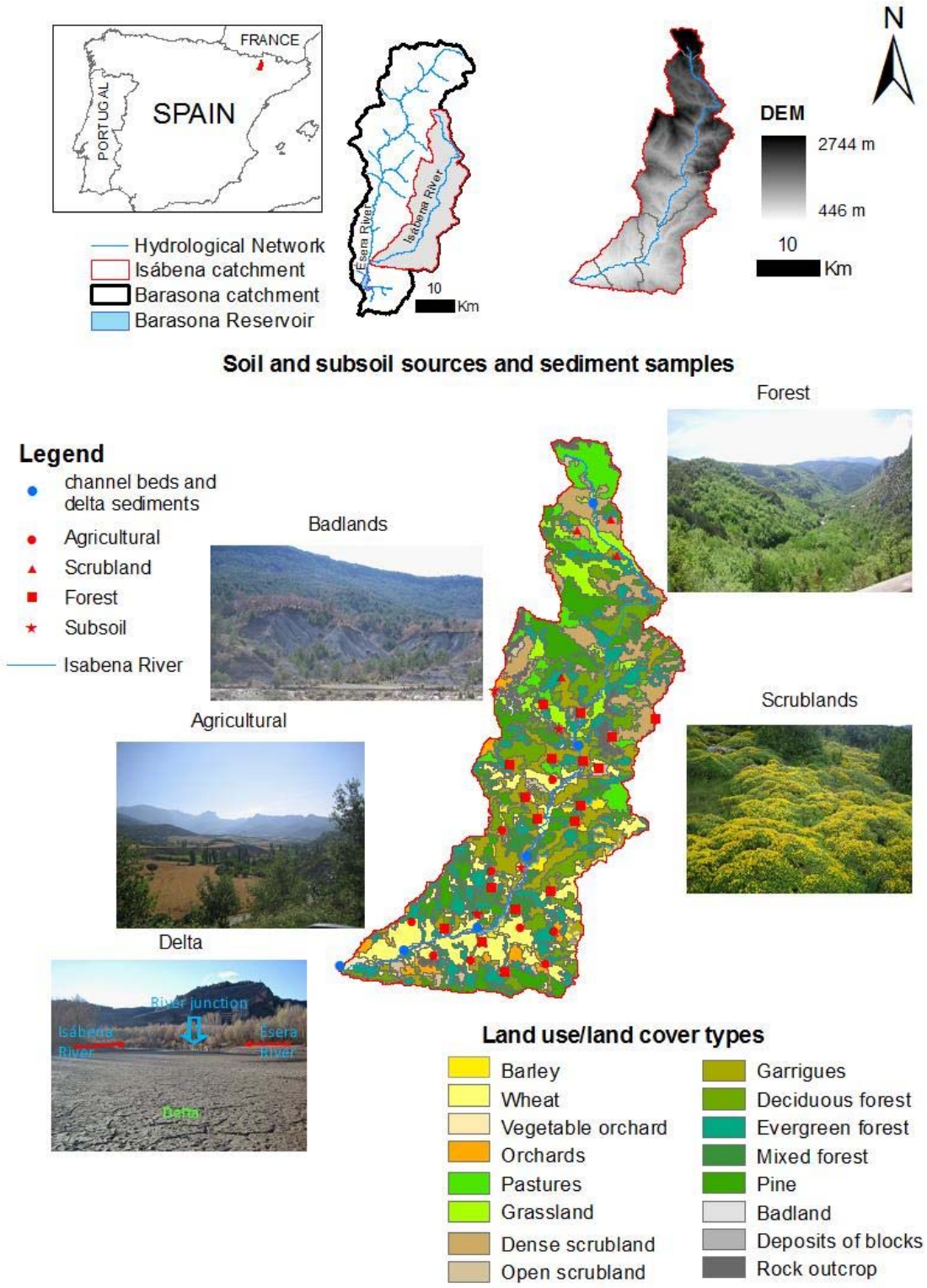

Fig. 2 Spatial distribution of source and target sediment samples in the contributing sub-catchments of the Isábena catchment for the soil types, lithology and land use/land cover maps (classes simplified from the digitalized map of the Project Corine Land Cover 2006)

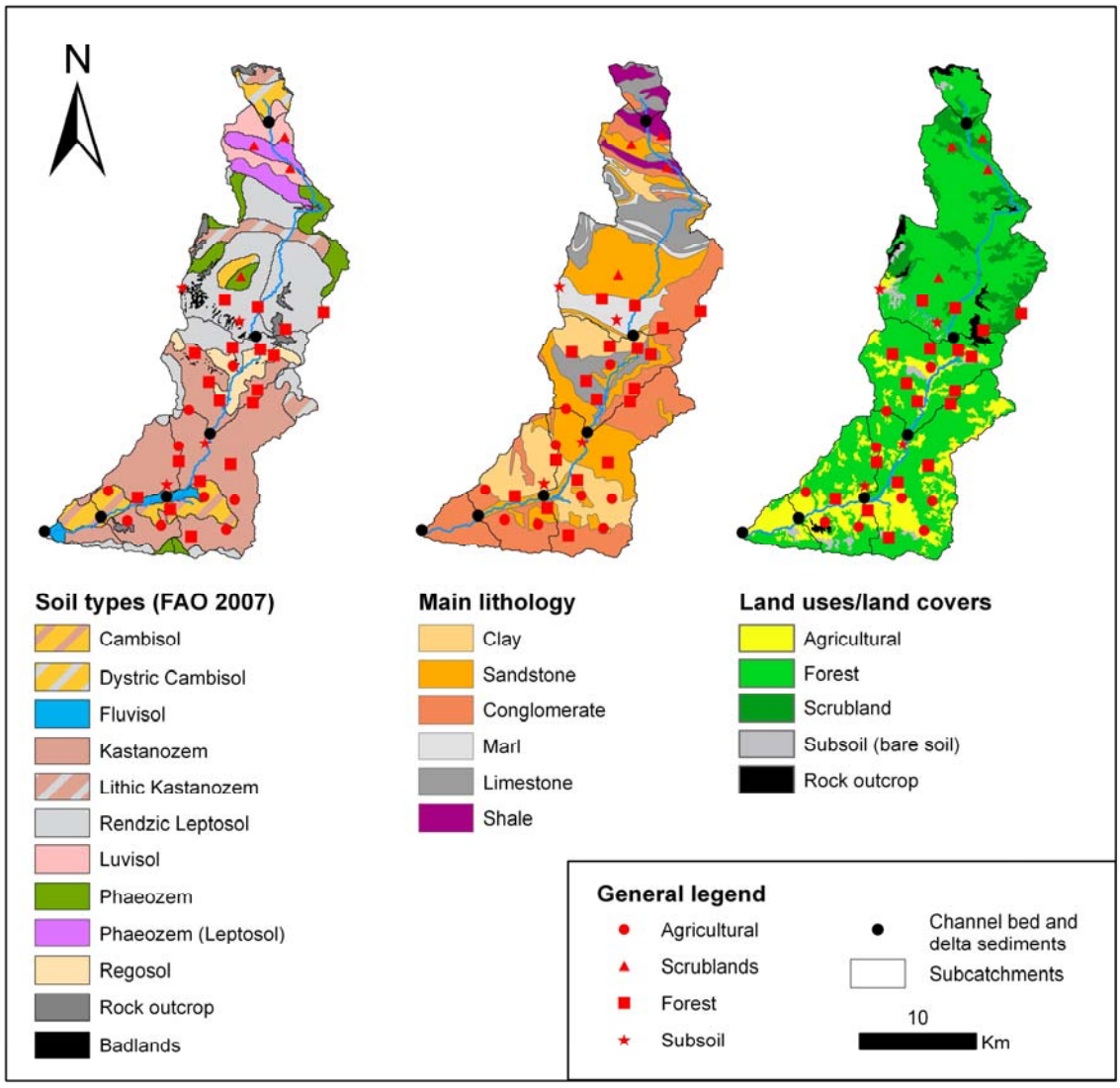

Fig. 3 Barasona reservoir levels

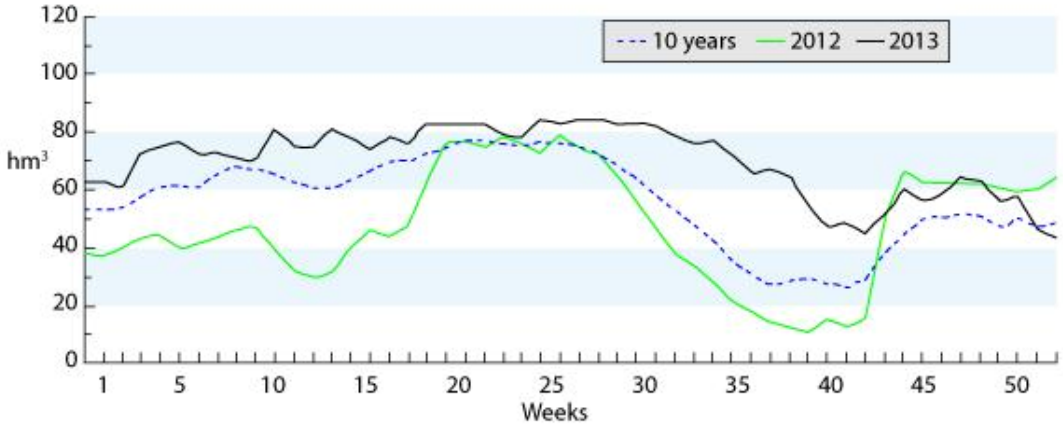

Fig. 4 Distribution of the grain size of sediments in the channel beds and delta sampling points in the Isábena catchment

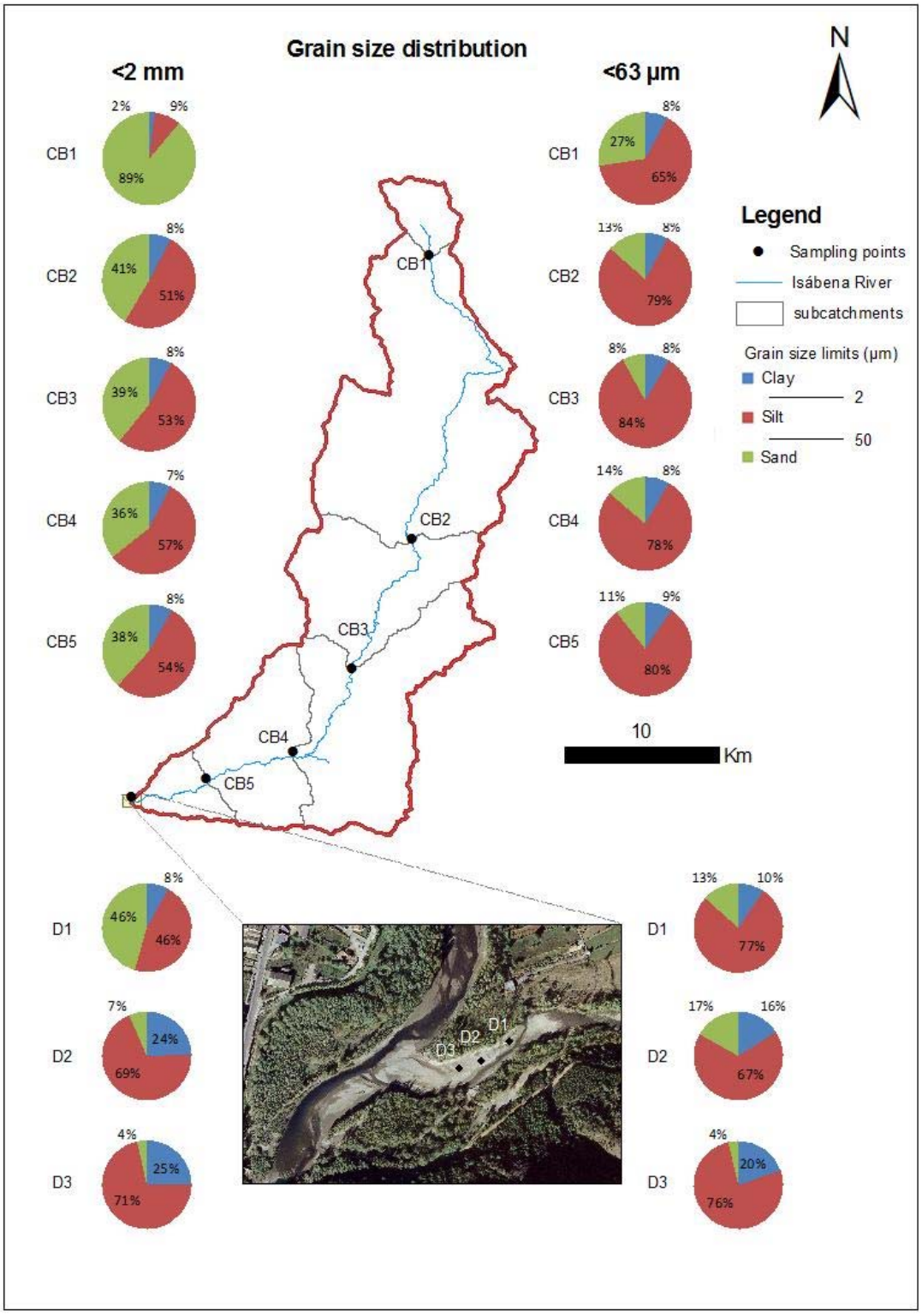

Fig. 5 Box plots of the tracer properties for the optimum composite fingerprint

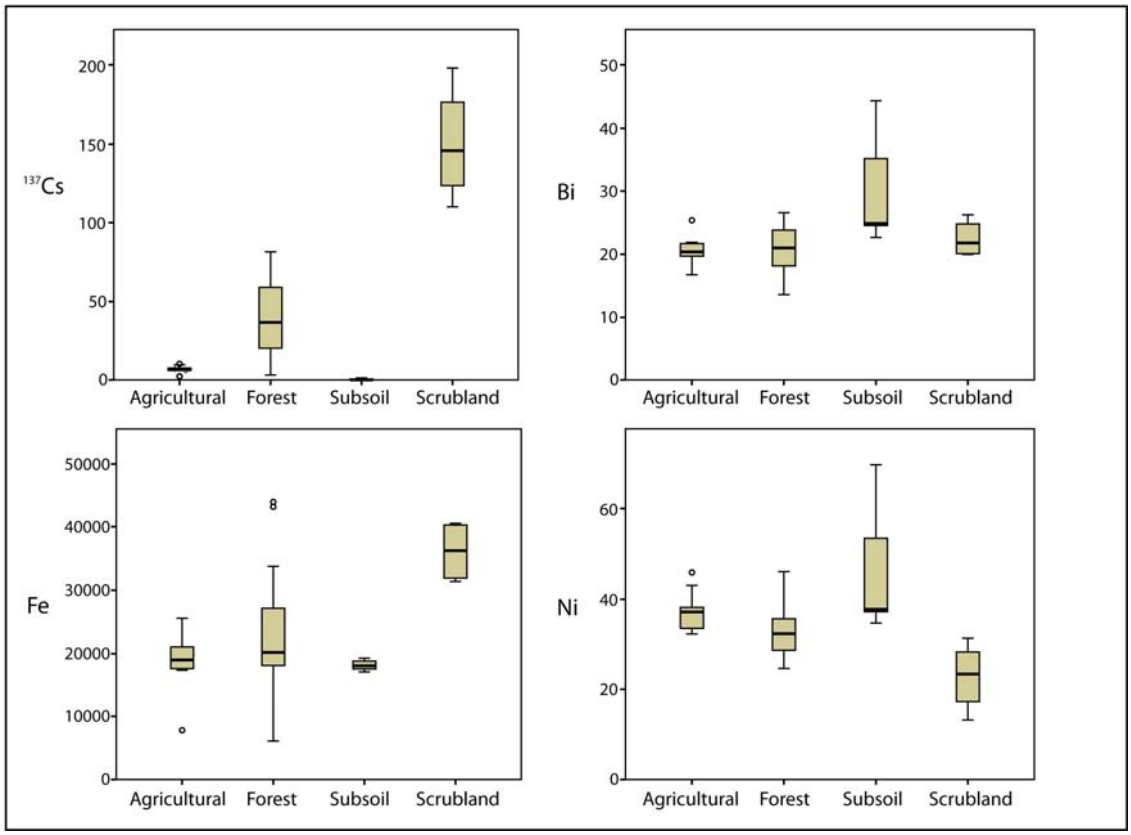

Fig. 6 Two-dimensional scatter plot of the first and second discriminant functions from the stepwise discriminant function analysis (DFA)